

Deep Learning Model with Enhanced Segmentation and Combined Feature Activation for Mitosis Classification

Jithy Lijo¹, Saleema J.S.², Tina Babu³

¹Department of Computer Science, ²Department of Statistics and Data Science, Christ University, Bengaluru, Karnataka, India.

E-mail: ¹jithy.lijo@gmail.com, ²saleema.js@christuniversity.in, ³tina.babu@alliance.edu.in

Abstract

Mitosis is a cell division mechanism vital for the growth of tissues and repair, Histopathological images are used by pathologists to diagnose cancer, but mitosis classification plays an important role in disease diagnosis. The mitotic counts are a proliferative indicator to find the aggressiveness of breast cancer. Detecting the mitotic tumor cells in tissue areas is a critical marker in cancer prognosis. Various researchers have focused on developing an automatic detection framework to identify mitotic figures, but detecting and classifying mitosis accurately remains a significant challenge in the medical field. Moreover, this research has designed a proposed Aggressive Tracing Seeking Optimization (ATSO) based Deep Convolutional Neural Network (Deep CNN) for the mitosis classification framework. The proposed framework uses less memory and increases the convergence rate; hence, it is globally efficient in achieving optimal solutions in the search space. The inspiration for considering the ATSO is its excellent behavior, as well as its scalable and adaptable mechanism, which allows optimization to move away from local optima. Moreover, it is computationally faster and exhibits higher global convergence capability in searching for the best solution. ATSO optimally trains a Deep CNN to generate higher classification accuracy by minimizing the false rate using the loss function. More explicitly, the proposed ATSO-Deep CNN model attained higher performance with an accuracy of 96.31%, an F1-score of 96.3%, precision of 96.84%, and recall of 95.78% with a 90% training percentage for the BreCaHAD dataset.

Keywords: Mitosis Classification, Histopathological Images, Cancer Prognosis, Deep Convolutional Neural Network, Feature Fusion, Segmentation.

1. Introduction

In recent decades, breast cancer has progressively amplified, and the age group affected by this disease has gradually decreased. It is also a leading cause of death among women, making the gradient an important measure for disease prognosis [1]. The Nottingham Grading System (NGS) states that there are three significant morphological features in the Hematoxylin and Eosin (H&E) slides used to grade breast cancer: mitotic count, nuclear pleomorphism, and tubule development [2]. According to the NGS, mitosis is the most important indicator, offering the strongest value among the three features. Achieving consensus on mitotic count among

¹School of Computer Applications, Dayanada Sagar University, Bengaluru, Karnataka, India.

³Alliance School of Advanced Computing, Alliance University, Bengaluru, Karnataka, India.

pathologists is very complex due to the subjectivity involved in identifying mitotic cells [3]. Mitosis is the process of nuclear division in living organisms, comprising four different phases: metaphase, anaphase, prophase, and telophase [4]. In the procedure of cancer staging and grading, cancer grading primarily detects the aggressiveness of cancer, while cancer staging indicates how far it has progressed from the primary organ to other parts of the body [5]. Mitosis detection serves as an index of the nuclear proliferation rate and is reported as the cancer class. Therefore, mitosis detection and recognition play an essential role in accurate diagnosis and grading systems, as well as in predicting effective treatment and survival [6]. Additionally, mitotic count estimation mostly relies on the persistent identification of nuclei in whole slide images (WSI). This identification is usually carried out by pathologists but is complex, timeconsuming, highly variable, and intensive. Therefore, it is essential to develop automated methods in computer-assisted systems for mitosis classification [7]. Automated detection techniques should aim to decrease time utilization, reduce labor costs, and minimize material resources, in addition to enhancing diagnostic dependability. To develop an automatic technique, one should first identify the nucleus and then properly identify mitosis in WSI. Several machine-learning techniques have been introduced for identifying mitotic cells in histopathological images [8] recently. Deep learning-based methods have attracted a lot of interest among scholars in the field of disease diagnosis, particularly breast cancer classification. The CNN model has made a tremendous contribution in many fields and has automated most of the medical system's important processes. It is extremely challenging to distinguish between normal partitions and mitotic partitions without high-resolution images and the intervention of pathologists since mitotic partitions have textures and morphological structures similar to those of normal partitions [9]. To understand the intricate structure of mitosis, the U-Net model was created with segmentation maps and achieved quicker segmentation using context-based learning. A series of advanced U-Net models have since been proposed, including Attention U-Net, Inception U-Net, Residual U-Net, Dense U-Net, U-Net++, and Adversarial U-Net, for different applications [10].

In the deep learning mechanism, the model fails to consider the weight transfer function to improve detection performance. In multi-task deep learning, the Mask Mitosis model was developed to detect mitosis with unlabeled and weakly annotated datasets, but it failed to consider a fully annotated dataset [11]. The artificial intelligence-based method obtained better performance but faced issues with computational cost. Moreover, it failed to use large datasets to evaluate the accuracy of breast cancer cases. The deep mitosis detection framework showed better detection results but failed to focus on generating accurate pixels for centroid annotations, which enabled training a powerful detector. The mitosis detection method designed in [12] performed well under small-sized datasets, but it does not consider large-sized datasets for analyzing performance. It does not consider the ensemble model in analyzing performance. The mitosis detection method in [13] analyzed performance without considering the features of the deep learning framework. It achieved substantial improvement in both reliability and accuracy, but determining the features resulted in a challenging task. To address the above limitations in existing techniques, the proposed model was developed. The proposed mitosis classification research utilizes effective preprocessing techniques, which overcome the noisy, low-contrast, and external artifacts in the input histopathological images. Further, the utilization of the ATSO algorithm with the U-Net model for segmentation selects the significant features using segmentation maps, which helps to focus on accurate mitosis classification. The proposed fused DpMIE-Net feature descriptor extracts the significant features from complex structures, enabling the optimized DCNN for accurate detection. The substantial contribution of this research is detailed as follows:

- Optimized U-Net-based Segmentation: The segmentation process with the U-Net model extracts deeper features from histological images, resulting in better performance for mitosis classification. The integration of the ATSO algorithm tunes the U-Net model for accurate segmentation with minimal errors.
- Fused DpMIE-Net Feature Extraction: The combination of Deep MobileNetV2, Inception-V3, and EfficientNet (DpMIE-Net) models in feature extraction extracts significant and complex features from the segmented image. The feature fusion mechanism increases the scalability and adaptability of the model, maximising the accuracy of classification.
- Optimized Deep CNN-based Classification: The Deep CNN generates the feature map at the convolution layer using different kernels. The ATSO optimization incorporates different aggressive behaviors that improve convergence, which directly impacts the Deep CNN model by reducing the computational cost and increasing training speed.

The rest of the research paper is arranged as follows: Section 2 presents the problem statement Section 3 describes the model of the system. Section 4 elaborates on the results and experimentation details, and finally, Section 6 concludes the research.

2. Problem Statement

Different studies are analyzed to accurately detect the sample type in histopathology images. However, a variety of partition shapes, sizes, colors, and scales in the histopathological images make the detection task more complex. Moreover, the complex pattern of body partitions, the similarity between malignant and benign samples, and low-quality images with stain variations prevent the diagnosis mechanism from achieving higher accuracy. However, the dataset has a class imbalance issue with mitosis and non-mitosis samples, which is addressed by the loss function. Hence, the development of an effective deep learning model for the early diagnosis of mitosis will help patients minimize the severity of the disease at an early stage. Assume the image captured from the dataset, is used to detect normal or abnormal cases by passing the image through various stages, like pre-processing, segmentation, feature extraction, and d B etection.

$$D = \{B_1, B_2, ..., B_i, ..., B_n\}; 1 \le i \le n$$
(1)

The input images are processed effectively by eliminating external artifacts and are segmented by the classifier model, and it is represented as, S, that is further trained by the model to determine the optimal result. Further, the categorical cross-entropy loss is utilized to overcome the class imbalance issues, where weights are assigned for the minority classes to maintain the probability of each class. The loss function serves as the indicator used to determine the performance of the learning mechanism in predicting accurate results. Here, categorical cross-entropy is considered the loss function to analyze the performance of this model.

$$L = -\log\left(\frac{e^{s}}{\sum_{j=1}^{J} e^{g_{j}}}\right)$$
(2)

Here, L is the loss function, J denotes the number of classes, S denotes the positive score of the model, and S_j specifies the probability of the minority class. Each image undergoes all the stages, and finally, the optimized network performs the detection mechanism to determine whether the image is normal or abnormal.

3. Proposed Methodology

The early diagnosis of breast cancer significantly minimizes the mortality rate. For early diagnosis, mitotic count plays an important role in predicting the prognosis, aggressiveness, and grade. This research designs the ATSO-based Deep CNN model for the detection and categorization of mitosis. The input image is sourced from the histopathological image dataset that undergoes a pre-processing phase, where Gaussian blur and median filters are applied to improve the quality of the image. The quality-enhanced image is taken to the image segmentation module, in which an optimized U-net is implemented to generate the segmentation results. The segmented image is passed to feature extraction, where DpMIE-Net is used to capture the features independently and fuse them to generate the feature vector. The feature map is fed to a Deep CNN tuned with ATSO optimization, where the input feature vector is classified as mitosis or non-mitosis. Figure 1 illustrates the schematic view of the proposed method.

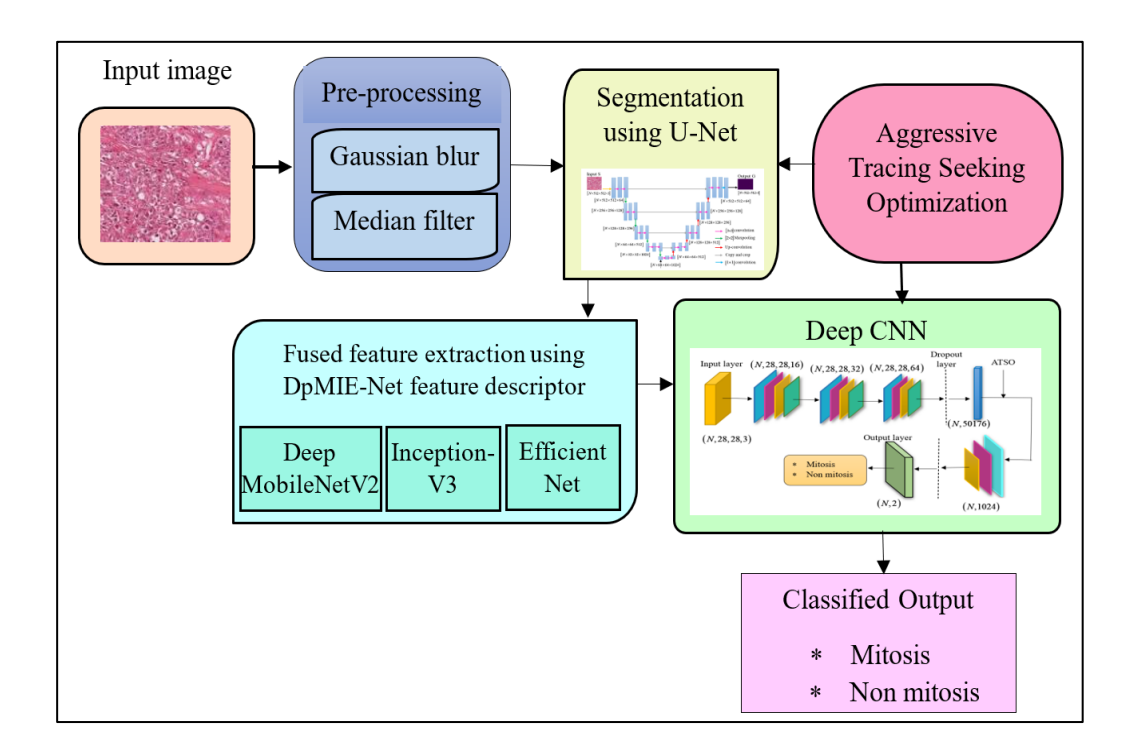


Figure 1. Workflow Diagram of the Proposed ATSO-based Deep CNN Model

3.1 Input Image Collection

The input histopathological images are acquired from the MITOS-ATYPIA-14 [14] and the BreCaHAD dataset [15]. However, these images are used to diagnose the disease in its initial phase, which aids in improving the rate of survival of human beings. Consider the dataset as *D* with *n* number of histopathological images and it is modeled as,

$$D = \{B_i\}; i \in \{1, ..., n\}$$
(3)

Here, B_i implying the image is placed at i^{th} index in the dataset.

3.2 Image Pre-processing

The Input image B_i undergoes the pre-processing phase, where the Gaussian blur and median filter methods are utilized to remove noise, external artifacts, and rectify the low-contrast in the input images, which effectively increases the quality of the image compared to other denoising techniques. These techniques will enhance the input images with good quality, making them more suitable for further processing.

Gaussian blur: It is the filter commonly used to smooth the given image B_i . The Gaussian blur [16] method generates a preprocessed image by smoothing the input image through the application of the Gaussian function to minimize the noise level. In general, this is accomplished by convolving the image with a Gaussian kernel, modeled as,

$$G(a,b,\sigma) = \frac{1}{2\pi\sigma^2} e^{-\frac{a^2+b^2}{2\sigma^2}} \tag{4}$$

Here, a and b are location indices, σ represent standard deviation and G denote a Gaussian kernel.

Median filter: It serves as the non-linear model used to remove noise from images by replacing each pixel value with the median value. It is a type of filter that uses a square-shaped window with an adjustable size to perform the filtering process [17]. The pre-processed image is denoted as S that is filtered by applying the pre-processing mechanism, and it is shown below,

$$S = PP(B_i); i \in \{1,...,n\}$$
 (5)

Here, PP is referred to as the pre-processing phase, which includes a Gaussian blur and a median filter mechanism to eliminate noise that exists in images, and the resulting image is represented as S having the dimension of $[N \times 512 \times 512 \times 3]$, which is further sent for segmentation.

3.3 Image Segmentation

The medical image segmentation process is crucial for complex anatomical structures, and previous research has faced difficulties in achieving accurate segmentation. However, U-Net has a deep learning architecture and is effective for accurate segmentation of complex

medical images. U-Net segmentation extracts deeper image features from histological images. Hence, U-Net is utilized in the proposed ATSO-Deep CNN model for segmentation, which leads to accurate mitosis classification. Furthermore, the incorporation of the ATSO algorithm tunes the parameters of U-Net for accurate segmentation. Segmentation is an image processing method used to separate the image into several regions, and it also refers to the process of specifying boundaries among separate semantic entities of the image. It is the procedure of assigning a label to every pixel in an image in such a way that pixels with the same labels are linked together based on some semantic property. The pre-processed image S is passed into a segmentation mechanism, where the U-Net model [10] is applied to determine the segmented image G. U-Net plays an essential role in the area of image analysis in medical research. The major purpose of using the U-Net model is that images with fixed dimensions are reduced to make the size of the image more visible in the display area and to create thumbnails of consistent images for extracting deeper image features. It is mainly modeled with up-sampling and down-sampling layers, and holds two different paths, the contracting path and the expansive path. Accordingly, up-sampling is employed to enlarge an image, and the features obtained from each layer of up-sampling and down-sampling are fused through a copy or crop mechanism. Each block located in the contracting path contains two successive convolutions with a specific size $[3\times3]$, a ReLU activation, and a maximum pooling layer. However, the structural arrangement is continuous for a number of times, and more novelty of this structure exists in an expansive path, and here, at every stage, the feature maps are upsampled by $[2\times2]$ convolution. Accordingly, the feature map obtained from a respective layer of the contracting path is allowed to crop and concatenate, and further, it is used with a feature map placed at the up-sample layer, followed by this, [3×3] convolution and a ReLU activation is employed. A [1×1] convolution is used to minimize the feature map to a number of channels and generate segmented results, which is represented as, G having a dimension $[N \times 512 \times 512 \times 3]$. Accordingly, the energy function is calculated pixel-wise at the softmax layer using the crossentropy loss function given as,

$$CE = \sum w(x) \cdot \log P_c(x) \tag{6}$$

$$P_{c}(x) = \frac{\exp(A_{c}(x))}{\sum_{c'=1}^{C} \exp(A_{c'}(x))}$$
(7)

Here, w(x) denotes the weight map, $A_c(x)$ implies activation in the feature channel c at pixel position x, $P_c(x)$ specifies the approximated maximum function, and c' is the true label of each pixel. The major benefit of using the U-Net model is that it contains a greater number of feature channels on the upsampling side, which allows the network to broadcast contextual details to the higher resolution layers. The U-Net is more effective in solving medical segmentation issues, and it effectively performs segmentation for large images. Figure 2 shows the architecture of the U-Net model [10].

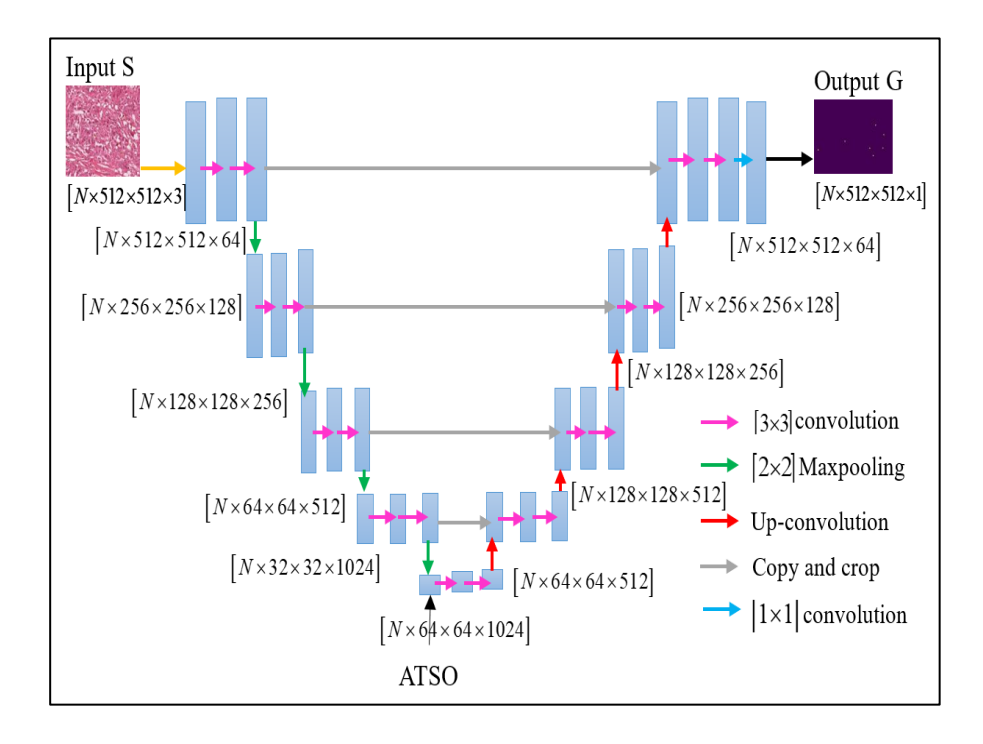


Figure 2. Architecture of the U-Net Model

3.4 Fused Feature Extraction

The segmented G as input and performs a feature extraction strategy, where optimal features are effectively captured to determine mitosis detection. In this, the DpMIE-Net feature descriptor employed three feature extraction mechanisms, such as Deep MobileNetV2, Inception-V3, and EfficientNet, for effective feature extraction. Further, these models extract more discriminative features from complex structures and fuse them to generate more significant features that enhance mitosis classification. The fused feature extraction process captures intricate patterns from the segmented results that are used to form a feature vector. This feature vector is then used by the classifier for recognizing mitosis classification.

3.4.1 Deep MobileNet Version 2

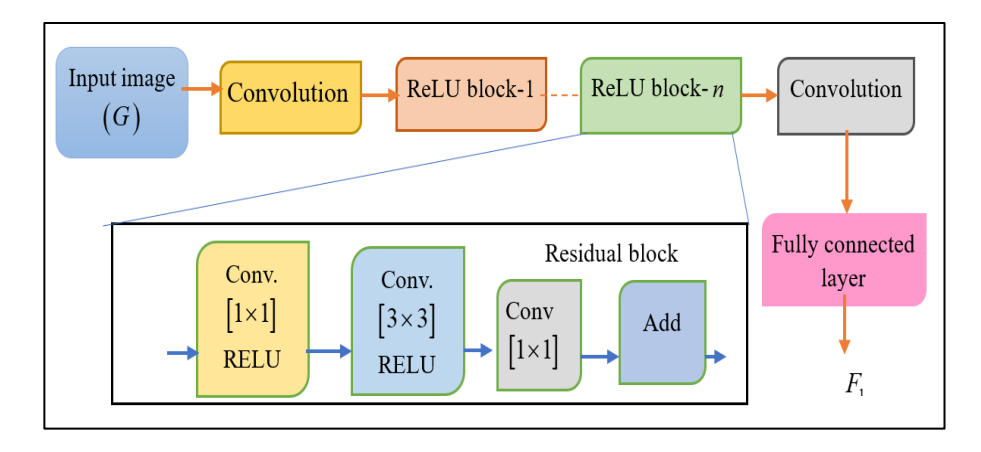


Figure 3. Architecture of MobileNetV2

The structure of Deep MobileNetV2 [18] is based on the depth-wise separation of convolutional layers. Here, standard convolution is used to process the input image directly for generating output features. After generating a filtered output channel, these channels are stacked and filtered using $[1\times1]$ convolution to integrate the stacked results into a single channel. The process of depth-wise convolution is similar to standard convolution, but the advantage of depth-wise convolution is that it minimizes the number of parameters used in the process. However, it takes the input G with dimension $[N\times512\times512\times3]$ pixels and generates the feature map as output F_1 with dimension $[N\times28\times28]$, respectively. Figure 3 explains the architecture of MobileNetV2.

3.4.2 Inception-Version 3

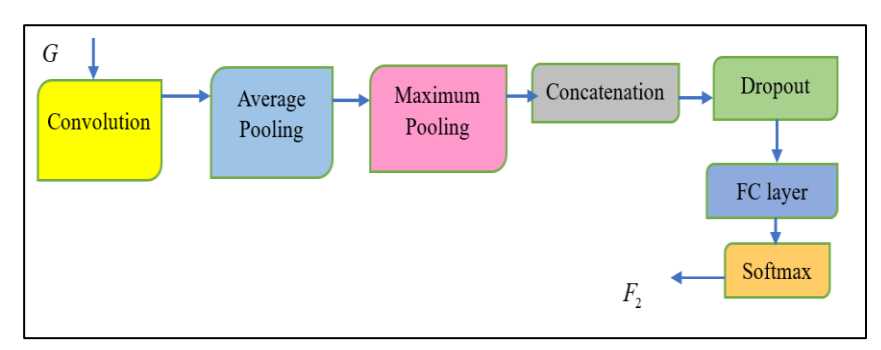


Figure 4. Architecture of Inception-V3

On the other hand, the segmented result G is fed as input to the Inception V3 model for generating the feature map. Inception-V3 [19] is a deep-learning network used to generate better feature maps by solving overfitting issues. The major benefit of using this feature mechanism is that it employs convolution $[1\times1]$ to minimize the number of feature channels and increase training speed. It takes the input of segmented images G with size $[N\times512\times512\times3]$ and computes the feature map F_2 with dimensions $[N\times28\times28]$ by involving different layers, like pooling, concatenation, dropout, and fully connected layers. Each layer performs its functions and generates the output feature map with reduced dimensionality. Figure 4 shows the structure of Inception-V3.

3.4.3 EfficientNet

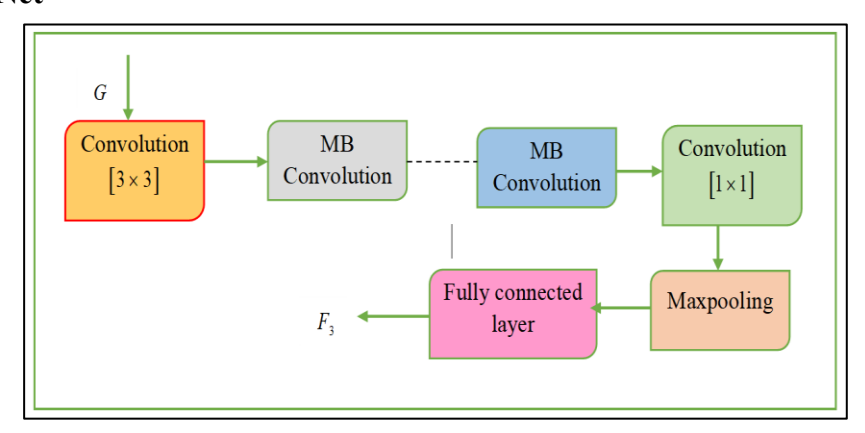


Figure 5. Structure of EfficientNet

The Efficient Net takes the input as G with size $[N \times 512 \times 512 \times 3]$ and computes the feature map as F_3 with size of $[N \times 28 \times 28]$, respectively. The efficient Net model [20] is an effective learning mechanism utilized to generate a feature map by reducing the number of channels. Accordingly, the benefit of using this network is the use of mobile inverted bottleneck (MB) convolution in depth which eventually minimizes the kernel size. Figure 5 illustrates the structure of EfficientNet.

More specifically, the features extracted through Deep MobileNetV2, Inception-V3, and Efficient Net have dimensions $[N \times 28 \times 28]$ that are concatenated as feature vectors. This process helps improve performance by reducing dimensionality and noise from the input images.

Finally, the feature vectors extracted from the Deep MobileNetV2, Inception-V3, and Efficient Net models are concatenated to generate significant features, expressed as,

$$F = \{F_1 \|, F_2 \|, F_3 \|\}$$
 (8)

Here, Deep MobileNetV2, denoted as F_1 , Inception-V3 as F_2 and Efficient Net as F_3 , F implying a feature vector with the size of $[N \times 28 \times 28 \times 3]$, further used to detect mitosis.

3.5 Optimized Deep Convolutional Neural Network for Mitosis Classification

The features extracted from the models are integrated and fused into a feature vector F that is given as input to the Deep CNN for classifying mitosis as normal or abnormal. The deep CNN [21] model effectively learns and extracts higher levels of features that can differentiate among various class labels in the classification scenario. The internal functions are performed in the hidden layer, which is typically composed of various convolutional, pooling, and fully connected layers. Here, extra layers are utilized to learn complicated features in order to achieve a proper decision strategy. The input layer takes the feature vector F as input with a dimension of $[N \times 28 \times 28 \times 3]$, which is further passed into the convolution layer with a dimension of $[N \times 28 \times 28 \times 16]$. The CNN architecture consists of 3 convolutional layers as well as 3 pooling layers built to extract features from a training set, using small filter with sizes of (16, 32, 64), and employs ReLU and softmax activation functions with one fully connected layer or dense layer. The output retrieved after applying the ReLU activation function to the convolutional layer is expressed as,

$$M = f\left(W * F + K\right) \tag{9}$$

Here, f is the function, W and K the weight and the bias. Further, the features are applied using the batch normalization technique to improve convergence speed for training the model. Then, the max pooling layer is considered to limit the dimension of the feature map while preserving confidential information. The max pooling output is sent to the next convolutional layer with a dimension of $[N \times 28 \times 28 \times 32]$, and the process continues for multiple layers. Then the dropout layer receives features with defined dimensions, $[N \times 28 \times 28 \times 64]$, which removes the irrelevant features during training, preventing overfitting issues in the model. A flattened layer is used to reduce the dimension $[N \times 50176]$. The dense

layer receives features with a dimension of $[N \times 1024]$, and the proposed ATSO algorithm is applied in the dense layer, which tunes the parameters for accurate classification. Further, the features are passed through the ReLU activation function and batch normalization layer, which normalize the activations of the data and forward it to the dropout layer. The dense layer computes output classes based on the input value through the softmax activation function, and the output is mathematically specified as, O_p with the dimension of $[N \times 2]$, which shows two classes: mitosis or non-mitosis. Accordingly, the loss function used to analyze the model's performance of in predicting results is specified in Eq. (2). the training procedure of this model is conducted by the ATSO algorithm that trains the hyperparameters, reducing the error rate and enabling the achievement of the global best solution. Figure 6 demonstrates the structure of the Deep CNN.

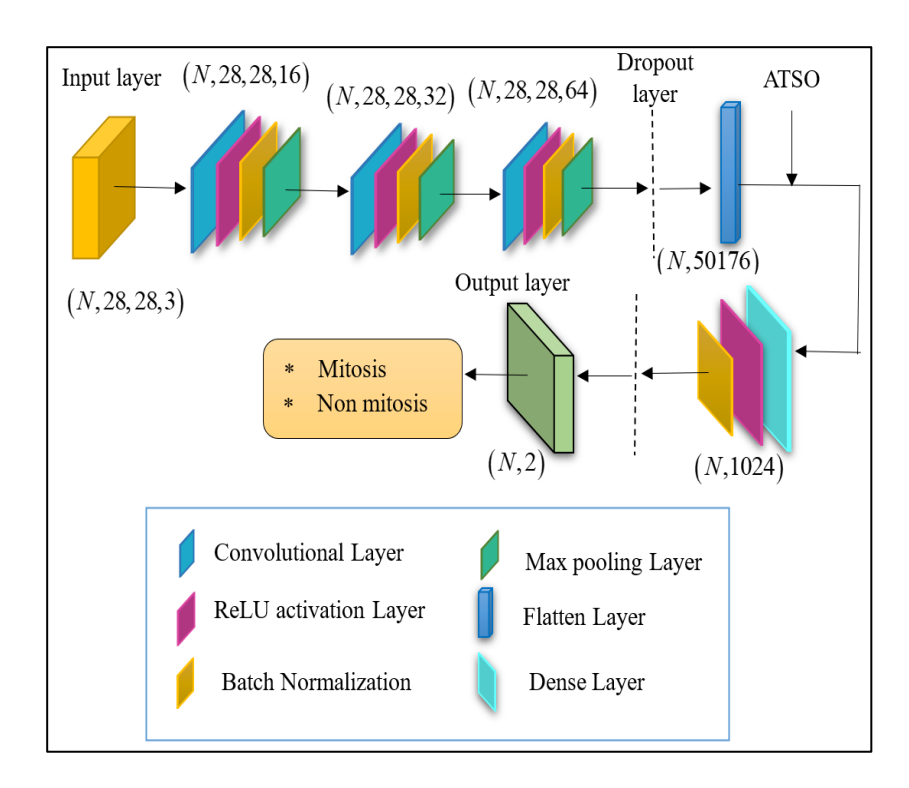


Figure 6. Architecture of an Optimized Deep CNN for Mitosis Classification

3.5.1 Aggressive Tracing Seeking Optimization

The proposed ATSO algorithm is developed through the integration of the seeking and tracing characteristics of Cat Swarm Optimization (CSO) [22] with the chasing and fighting behavior of Rat Swarm Optimization (RSO) [23], respectively. These behaviors are very aggressive and highly effective in solving optimization issues and avoiding convergence towards a local optimum. However, these behaviors are the major motivation for building the optimization model for tuning the U-Net model and Deep CNN model for accurate mitosis segmentation and classification, which also reduces false errors and enhances the convergence rate. The mathematical formulation of tuning the model to achieve high accuracy is explained as follows.

Initialization: The initialization is made chaotically with the enhanced mechanism, where the parameters can prevent the model from falling into the local minimum solution [22].

The optimization is built as to be unpredictable with a random nature, providing an easy and faster way of generating and storing information. The random solution is initialized in the search space, let us assume, $H_{u,v}$ as v^{th} dimension of u^{th} individual, and the chaotic map factor as Q. Hence, the chaotic sequence used to initialize the solution is mathematically modeled as,

$$H_{u,v}^{m} = H_{u,v\min} + Q_{v}^{m} \left(H_{u,v\max} - H_{u,v\min} \right); u \in \{1,...,U\}, v \in \{1,...,V\}$$
(10)

Here, $H_{u,v\min}$ shows the lower bound factor, $H_{u,v\max}$ represents the upper bound factor, Q_v^m represents the chaotic map at m^{th} iteration, U indicates population size, and V indicates total dimension.

Fitness function: In this algorithm, the fitness function is tuned to measure the high accuracy of the model in the classification process. The fitness function F_t is evaluated as,

$$F_{t} = Max \left[Accuracy \left(H_{u,v}^{m} \right) \right]$$
(11)

The maximum fitness value or maximum accuracy defines the solution to attain the global best value by eliminating the local optima.

Solution Update: To find the optimal solution, the random solution is classified based on the characteristics of rat and cat optimization, which is explained in the following section.

Case (i) Quick search phase: If $||H_{u,v}^m|| \in T$ satisfied, the quick search phase is activated by inheriting the resting characteristic features of rats and seeking the characteristics of cats. The updated solution at this phase is given as,

$$H_{u,v}^{m+1} = \frac{1}{2} \left[H_{u,v}^{m} \left(1 + R_1 * R_2 + X - Y + Y H_{best} \right) \right]$$
 (12)

$$H_{u,v}^{m+1} = \frac{\left(1 + R_1 * R_2\right) H_{u,v}^m}{2} + \frac{1}{2} \left[\left(X \cdot H_{u,v}^m\right) + Y \left(H_{best} - H_{u,v}^m\right) \right]$$
(13)

$$H_{u,v}^{m+1} = \frac{1}{2} \Big[\Big(1 + R_1 * R_2 \Big) H_{u,v}^m + X \cdot H_{u,v}^m + Y \Big(H_{best} - H_{u,v}^m \Big) \Big]$$
(14)

$$R_{1} = \left| \frac{F_{t}(H_{u,v}^{m-1}) - F_{t}(H_{u,v}^{m-2})}{F_{t}(H_{u,v}^{m-1}) + F_{t}(H_{u,v}^{m-2})} \right|$$
(15)

$$X = R_3 - m \left(\frac{R_3}{m_{\text{max}}} \right) \tag{16}$$

$$Y = 2.rand()$$
 (17)

where R_1 shows the fitness measure of the current and previous value and it lies between 0 and 1, R_2 denotes seeking range of selected dimension, m specifies current iteration, m denotes the maximum iteration, X and Y are the parameters, and rand denotes the random number.

Case (ii) Aggressive tracking phase: If $||H_{u,v}^m|| \notin T$ satisfied, the aggressive tracking phase begins by incorporating the fighting behavior of rats and tracing the character of cats. The position update solution of cat is defined as,

$$H_{u,v}^{m+1} = H_{u,v}^m + Z_{u,v}^m \tag{18}$$

Here, $Z_{u,v}^m$ is the velocity at the previous iteration.

The fighting behavior of rats is given as,

$$H_{u,v}^{m+1} = \left| H_{best} - (X.H_{u,v}^m) + Y(H_{best} - H_{u,v}^m) \right|$$
(19)

With Eq. (18) and Eq. (19), the position update solution at this phase is modeled as,

$$H_{u,v}^{m+1} = \frac{H_{u,v}^{m} + Z_{u,v}^{m} + \left| H_{best} - \left(X.H_{u,v}^{m} \right) + Y \left(H_{best} - H_{u,v}^{m} \right) \right|}{2}$$
(20)

$$Z_{u,v}^{m} = Z_{u,v}^{m-1} + y.z(H_{best} - H_{u,v}^{m})$$
(21)

Here, H_{best} denotes the best search agent, $y = e^{-\frac{m}{m_{max}}}$ and its value lies between [0,1] and z is a constant value.

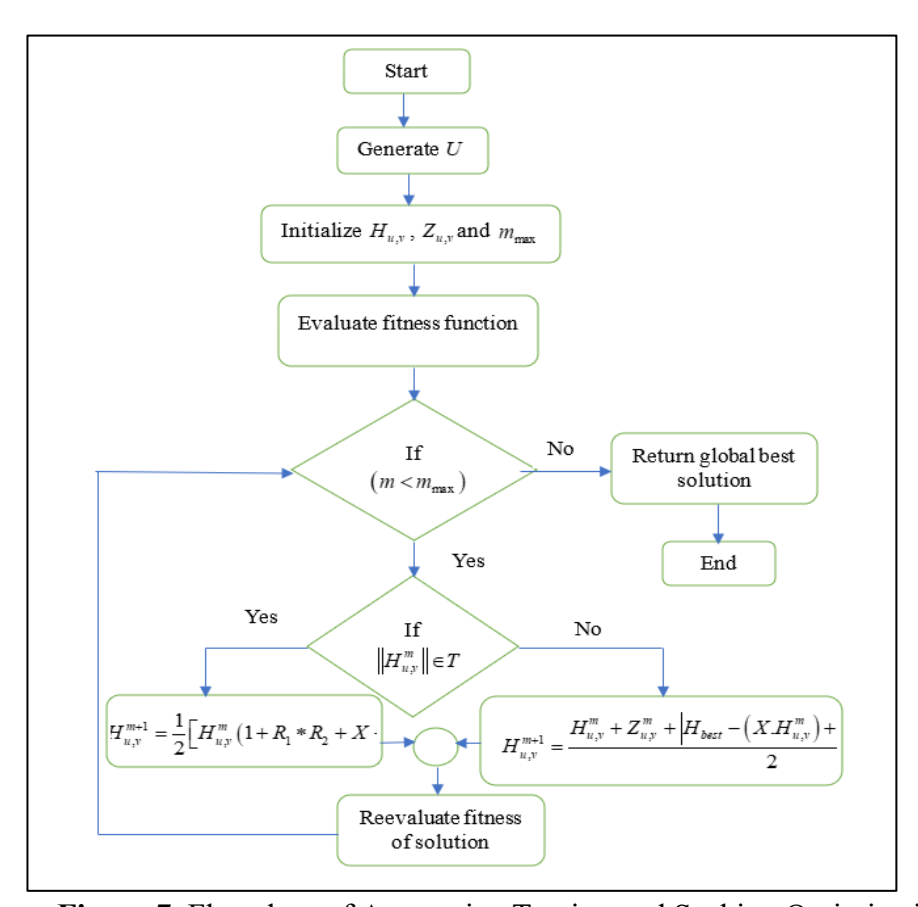


Figure 7. Flowchart of Aggressive Tracing and Seeking Optimization

Termination: The fitness function is evaluated for each result at every single iteration to find high accuracy, and the optimization continues until the best result is obtained. After reaching the best solution, the iteration is terminated. The ATSO trains the hyperparameters of the model to determine optimal solutions for mitosis classification with a high convergence rate and minimum misclassifications. Figure 7 shows the flowchart of the ATSO algorithm.

4. Results and Discussion

This division demonstrates the results as well as a discussion of the ATSO-Deep CNN model by showing the improvement of the deep learning model through analysis with existing methods.

4.1 Experimental Setup

The research on mitosis detection using the ATSO-Deep CNN model is executed in PyCharm software with the Python 3.7 programming language, which requires Windows 11 OS, 16 GB of RAM, 128 GB of ROM, an Intel i7-13770K processor, and 12GB of GPU memory. The initial parameter settings involve a batch size of 32, learning rate of 0.001, 500 epochs, a dropout rate of 0.5, an activation function of 'linear', a loss function of 'MSE', 45 LSTM units and the default optimizer Adam. The input data is split with a 90:10 ratio for return rate prediction, where 90% is used for training and 10% for testing purposes.

4.2 Dataset Description

MITOS-ATYPIA-14 dataset [14]: The dataset comprises a set of breast cancer biopsy slides collected from the Pitié-Salpêtrière Hospital in Paris, which contains 284 frames at X20 magnification and 1,136 frames at X40 magnification. These pathological images are stored in CSV file format with frames of RGB bitmap images in TIFF format. Furthermore, the frames at X20 magnification are subdivided into four different frames of X40 magnification, which are used for annotating mitosis. The dimensions of the X20 frame are 1539×1376 pixels, and the size of the magnification located inside tumors is 755.649×675.616 µm². The X40 frames are annotated as mitosis or not mitosis by three pathologists. Likewise, nuclear atypia is categorized into six types, size of nuclei, size of nucleoli, density of chromatin, thickness of nuclear membrane, regularity of nuclear contour, and anisonucleosis.

BreCaHAD dataset [15]: The dataset, called the Breast Cancer Histopathological Annotation and Diagnosis dataset (BreCaHAD), contains 162 breast cancer histopathology images. This dataset is annotated into six classes based on their histological structures; mitosis, apoptosis, tumor nuclei, non-tumor nuclei, tubule, and non-tubule. This diagnostic dataset has 492 files in 2 columns, stored in 1.06GB. The BreCaHAD dataset contains microscopic biopsy images taken over a duration of 2 to 20 years and saved in (.TIFF) format, with RGB and 8-bit depth in the channels. The dimensions of the annotated images are 1360 × 1024 pixels, and the annotation data is given in JSON format. Also, this dataset includes four types of malignant breast cancer; ductal carcinoma (DC), lobular carcinoma (LC), mucinous carcinoma (MC), and tubular carcinoma (TC).

4.3 Experimental Results

The experimental results of the ATSO-Deep CNN model for the mitosis classification process are showcased in this section, which is illustrated in Figure 8.

Techn	iques	Sample 1	Sample 3		
Input		7			
Preprocessi ng Gaussian filter		Ī			
	Median filter				
Segmente	ed Image				
Feature extraction	MobileNet				
	Inception				
	EfficientN et				
Output			Sea Pilla		

Figure 8. Experimental Results for Mitosis Classification

4.4 Performance Metrics

The performance of the proposed ATSO-Deep CNN model is evaluated using metrics such as accuracy, F1-Score, precision, and recall, which are mathematically expressed as,

$$Accuracy = \frac{P_c}{P_T} \tag{22}$$

$$Precision = \frac{P_{cp}}{P_{cp} + P_{inp}}$$
 (23)

$$\operatorname{Re} call = \frac{P_{cp}}{P_{mp}} \tag{24}$$

$$F_1Score = \frac{2 \times \text{Pr} \, ecision \times \text{Re} \, call}{\text{Pr} \, ecision \times \text{Re} \, call}$$
 (25)

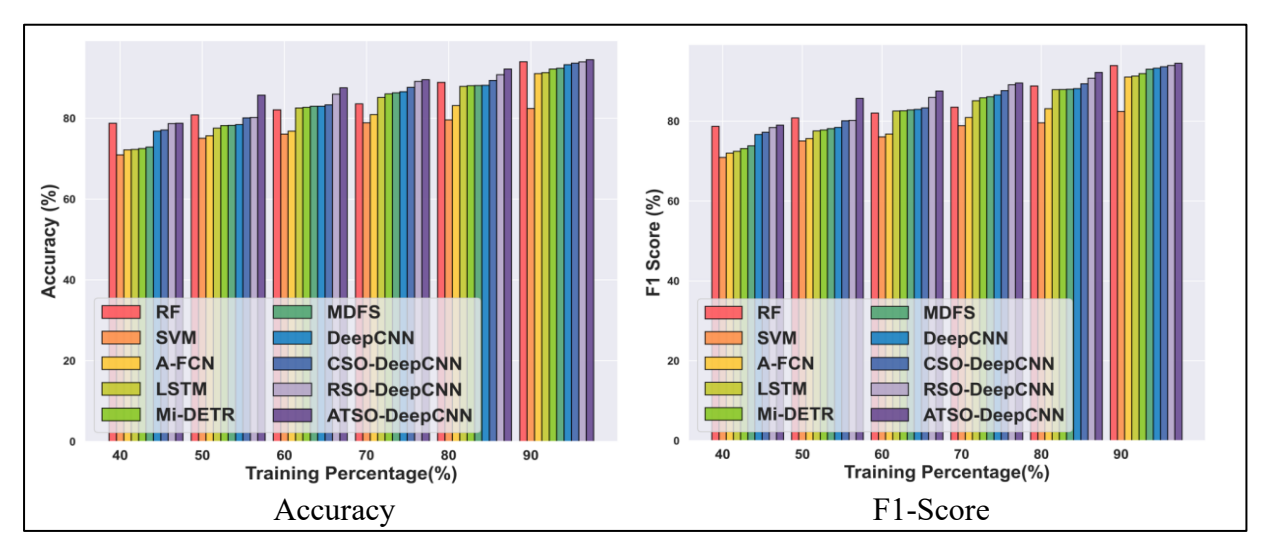
where, P_c is the correct prediction, P_T is the total prediction, P_{cp} is the correct positive prediction, P_{mp} is the missed positive prediction, P_{cn} is the correct negative prediction, P_{inp} and is the incorrect positive prediction.

4.5 Comparative Analysis

The performance of the proposed ATSO Deep CNN model for mitosis classification is evaluated against existing models, such as SVM [6], A-FCN [7], Random Forest (RF) [16], LSTM [24], Deep CNN [21], RSO-Deep CNN [23], CSO-Deep CNN [22], Mi-DETR [13], and MDFS based on various training percentages to enhance performance for mitosis classification.

4.5.1 Comparative Analysis with MITOS-ATYPIA-14 Dataset

Figure 9 shows the evaluation of the proposed ATSO Deep CNN model for mitosis classification using the MITOS-ATYPIA-14 dataset based on training percentages. At 90% training, the proposed model achieved high performance compared to other existing models. Moreover, the model achieved a high accuracy of 94.49%, which is 2.44% higher than the MiDETR model. Likewise, the proposed model's F1-score is 94.48%, which is 2.72% greater than the Mi-DETR model. Similarly, the model attained a precision of 95.28% and a recall of 93.7%, which are 2.22% and 3.21% greater than the Mi-DETR model.



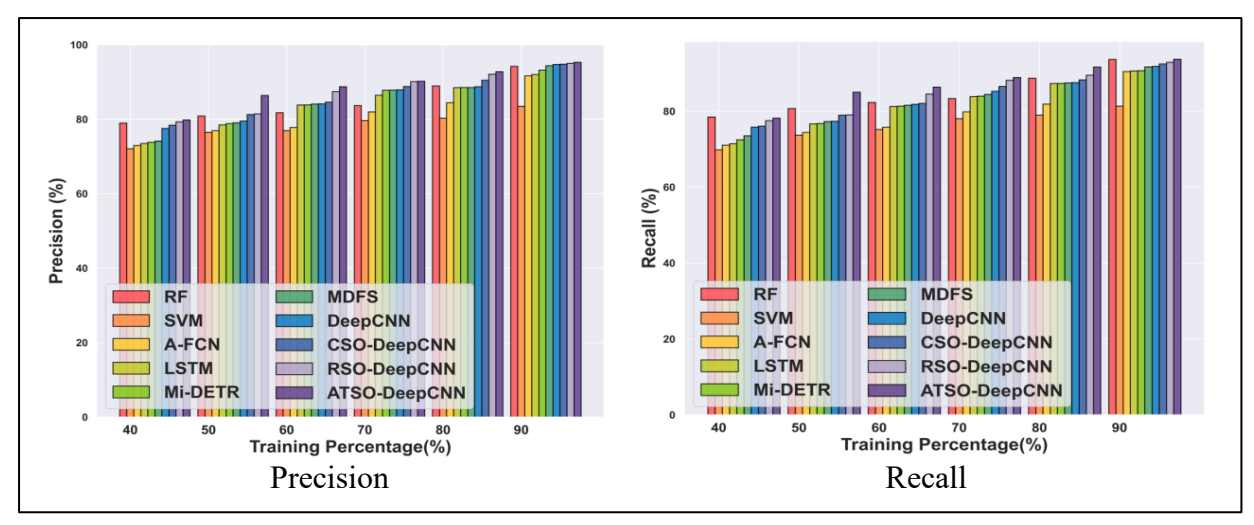
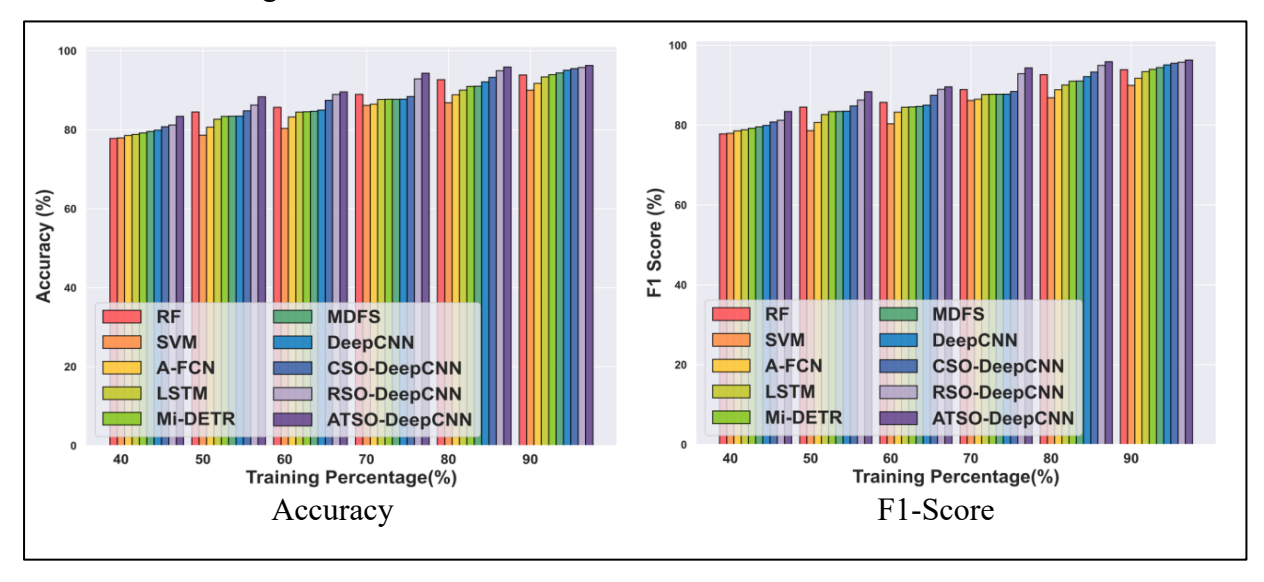


Figure 9. Comparative Analysis with the MITOS-ATYPIA-14 Dataset

4.5.2 Comparative Analysis with BreCaHAD Dataset

Figure 10 illustrates the evaluation of the proposed ATSO Deep CNN model for mitosis classification using the BreCaHAD Dataset based on various training percentages. At 90% of training, the proposed model achieved high performance and outperformed all the other existing models with an accuracy of 96.31%, which is 2.42% higher than the Mi-DETR model. Likewise, the proposed model's F1-score is 96.3%, which is 2.24% more than the Mi-DETR model. Similarly, the model attained a precision of 96.84% and a recall of 95.78%, which is 3.58% and 1.25% greater than those of the Mi-DETR model.



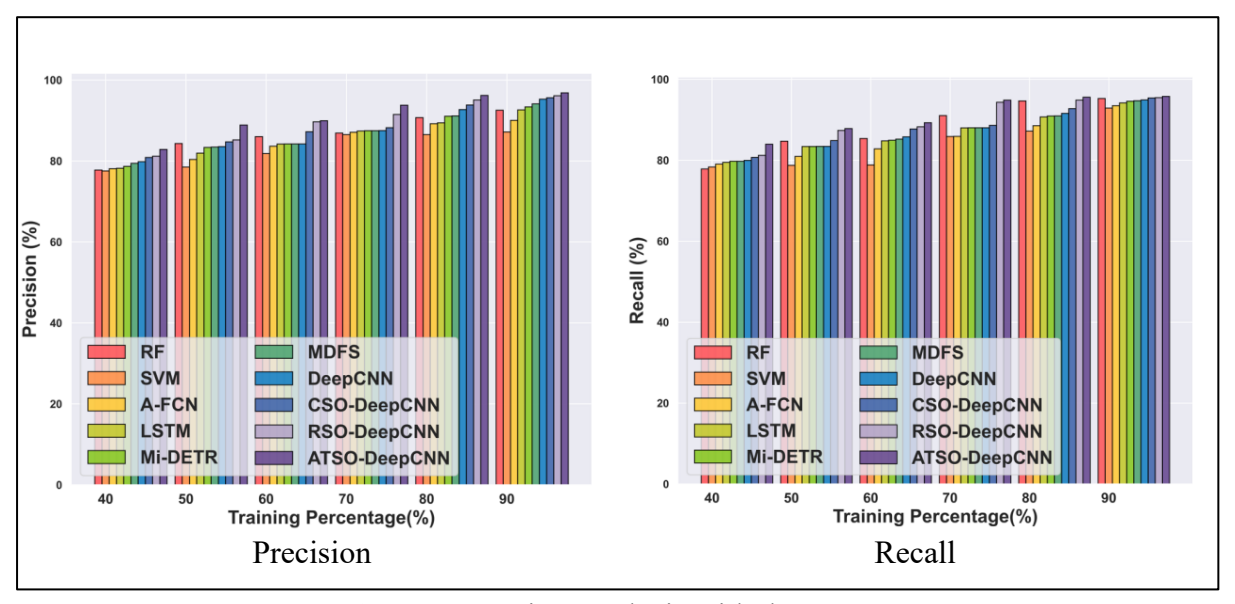


Figure 10. Comparative Analysis with the BreCaHAD Dataset

4.6 Comparative Discussion

The proposed ATSO-Deep CNN model is compared with other existing models to enhance the classification performance of the model. Generally, the conventional deep learning approaches used for mitosis classification attained better accuracy. However, those models have limitations such as complexity, time consumption, high computational cost, struggles with large datasets, and difficulty in complex feature extraction. Therefore, it is more important to design automated techniques in computer-aided systems for classifying mitosis. Most of the existing techniques obtained poor performance due to unbalanced data, computational issues, and noisy images, and failed to evaluate the mitosis level using the whole-slide image. Due to the above complex issues, the proposed ATSO-Deep CNN model is developed for classifying mitotic cells more accurately, which is highly suitable for medical research for the diagnosis of diseases with histopathological images. Here, the input histopathological image is preprocessed, and segments are formed to generate the features for mitosis classification. Moreover, a filtering approach is utilized for enhancing the image quality, from which the segments are formed using the U-Net model with the ATSO algorithm, such that the features acquired from the segments yield informative patterns for mitosis classification. Applying the feature fusion mechanism in the classification approach maximizes the accuracy of a classification and helps to learn images fully with their rich internal information. The inclusion of the DpMIE-Net features for feature fusion extracts intricate patterns from the input, which reduces the complexity of the model. The hybrid ATSO optimization fine-tunes the parameters of the proposed DCNN model to find optimal solutions with high accuracy, which increases the convergence rate with minimum loss. More specifically, the evaluation results show that the proposed model achieved high accuracy based on a large dataset of the MITOS-ATYPIA-14 dataset and the BreCaHAD dataset. Table 1 illustrates the comparative discussion of the ATSO-Deep CNN model.

Table 1. Comparative Discussion of the Proposed ATSO Deep CNN Model

Metrics/	MITO	S-ATYP	IA-14 dat	BreCaHAD Dataset					
Methods	Accuracy (%)	F1-score (%)	Precision (%)	Recall (%)	Accuracy (%)	F1-score (%)	Precision (%)	Recall (%)	
RF	93.97	93.91	94.19	93.64	93.91	93.89	92.54	95.27	
SVM	82.41	82.39	83.48	81.34	90.05	89.96	87.20	92.90	
A-FCN	91.05	91.05	91.65	90.45	91.77	91.74	90.05	93.49	
LSTM	91.31	91.30	92.00	90.61	93.40	93.40	92.62	94.18	
Mi-DETR	92.19	91.91	93.16	90.69	93.98	93.97	93.37	94.58	
MDFS	92.36	93.01	94.39	91.67	94.42	94.42	94.11	94.73	
Deep CNN	93.26	93.24	94.71	91.81	95.10	95.10	95.28	94.91	
CSO-Deep CNN	93.63	93.61	94.81	92.45	95.52	95.52	95.64	95.40	
RSO-Deep CNN	93.95	93.94	95.00	92.91	95.79	95.79	96.11	95.46	
ATSO Deep CNN	94.49	94.48	95.28	93.70	96.31	96.30	96.84	95.78	

4.7 Statistical T-test Analysis

The significance of the proposed ATSO Deep CNN model is evaluated based on statistical t-test analysis and compared with other existing models. The evaluation values show that the model attained p-values less than 0.05, indicating that the proposed model is statistically significant. Further, the statistical significance values are tabulated in Table 2.

Table 2. Statistical T-test Analysis

Models		RF	SVM	A-FCN	LSTM	Mi-DETR	MDFS	Deep CNN	CSO-Deep CNN	RSO-Deep CNN	ATSO-Deep CNN	
BreCaHAD Dataset	ıracy	T-statistic	2.55	3.79	2.85	3.70	3.72	3.69	2.98	3.22	3.16	4.11
	Accuracy	P-value	0.05	0.01	0.04	0.01	0.01	0.01	0.03	0.02	0.03	0.01

		T statistic	2.55	2.70	2.00	2.67	2.50	2.47	2.01	2 10	2 21	1.00
	F1-score	T-statistic	2.55	3.79	2.89	3.67	3.59	3.47	3.01	3.19	3.21	4.08
		P-value	0.05	0.01	0.03	0.01	0.02	0.02	0.03	0.02	0.02	0.01
	Precision	T-statistic	2.46	3.81	2.97	3.71	3.65	3.56	3.04	3.20	3.29	4.10
		P-value	0.06	0.01	0.03	0.01	0.01	0.02	0.03	0.02	0.02	0.01
	Recall	T-statistic	2.64	3.77	2.80	3.63	3.50	3.37	2.98	3.19	3.13	4.05
		P-value	0.05	0.01	0.04	0.02	0.02	0.02	0.03	0.02	0.03	0.01
MITOS-ATYPIA-14 dataset	Accuracy	T-statistic	3.90	2.64	3.10	3.42	3.39	3.30	3.18	3.44	3.83	3.81
		P-value	0.01	0.05	0.03	0.02	0.02	0.02	0.02	0.02	0.01	0.01
	F1-score	T-statistic	3.91	2.64	3.11	3.42	3.40	3.30	3.18	3.44	3.83	3.81
		P-value	0.01	0.05	0.03	0.02	0.02	0.02	0.02	0.02	0.01	0.01
	sion	T-statistic	4.05	3.10	3.35	3.47	3.49	3.28	3.06	3.34	3.66	3.97
	Precision	P-value	0.01	0.03	0.02	0.02	0.02	0.02	0.03	0.02	0.01	0.01
	Recall	T-statistic	3.75	2.18	2.80	3.36	3.28	3.31	3.30	3.54	3.92	3.61
		P-value	0.01	0.08	0.04	0.02	0.02	0.02	0.02	0.02	0.01	0.02

4.8 Segmentation Analysis

The proposed ATSO U-Net model is compared with existing models, such as MDFS, COADL-MNSC, W-UNET, U-Net++, Attention U-Net, and Trans U-Net, for the segmentation process. More specifically, the evaluation results show that the proposed ATSO U-Net model achieved an accuracy of 97.58% and outperformed the other models in segmentation. Further, the incorporation of the ATSO algorithm fine-tunes the U-Net for accurate segmentation. However, the existing models attain lower accuracy of 89.34% for MDFS, 91.86% for COADL-MNSC, 95.66% for W-UNET, 93.56% for U-Net++, 93.95% for Attention U-Net, and 96.57% for Tans U-Net. Further, the proposed ATSO-U-Net model achieved high performance in segmentation. The segmentation analysis for the proposed model is depicted in Figure 11.

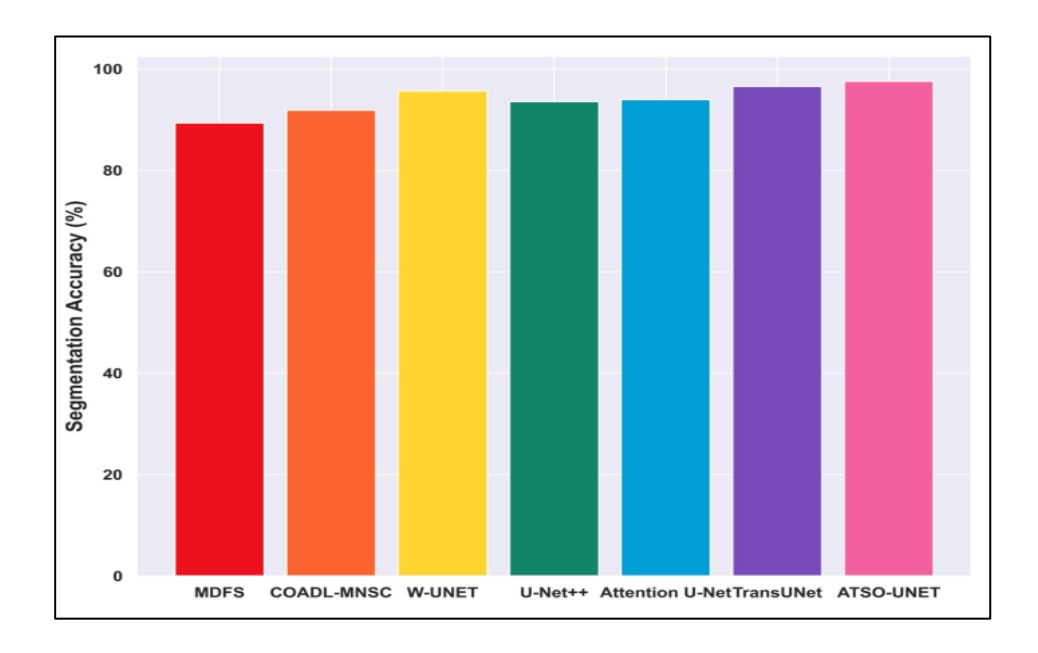


Figure 11. Segmentation Analysis

4.9 Confusion Matrix

The Confusion Matrix evaluates the performance of the proposed ATSO Deep CNN model and compares the predicted labels with actual labels to evaluate the model's classification performance. The high values of true positives (TP) and true negatives (TN) indicate that the model effectively identified mitosis and non-mitosis patients. The proposed ATSO Deep CNN model correctly classifies 5532 instances as mitosis and 5102 instances as non-mitosis with fewer misclassifications, such as incorrectly identifying 132 instances as non-mitosis and 131 instances as mitosis. Moreover, the proposed ATSO Deep CNN model provided robust results for mitosis classification. However, these misclassifications can have consequences in real-world applications, such as incorrect diagnosis, which may delay cancer treatment and increase the intensity of the disease. Figure 12 represents the confusion matrix of the proposed model.

4.10 Computational Complexity

The computational complexity explains the amount of time taken for the ATSO algorithm for segmentation and classification of mitosis. The proposed ATSO Deep CNN model utilized less computation time of 20.59s compared with other existing models, which enabled high-speed computation with minimal loss. The execution time required for the existing models is as follows: RF of 20.83s, SVM of 20.60s, A-FCN of 20.64s, LSTM of 20.72s, Mi-DETR of 20.72s, MDFS of 20.74s, Deep CNN of 20.80s, CSO-Deep CNN of 20.80s, and RSO-Deep CNN of 20.81s. Which is higher compared with the proposed model. Figure 13 demonstrates the computational complexity of the proposed model.

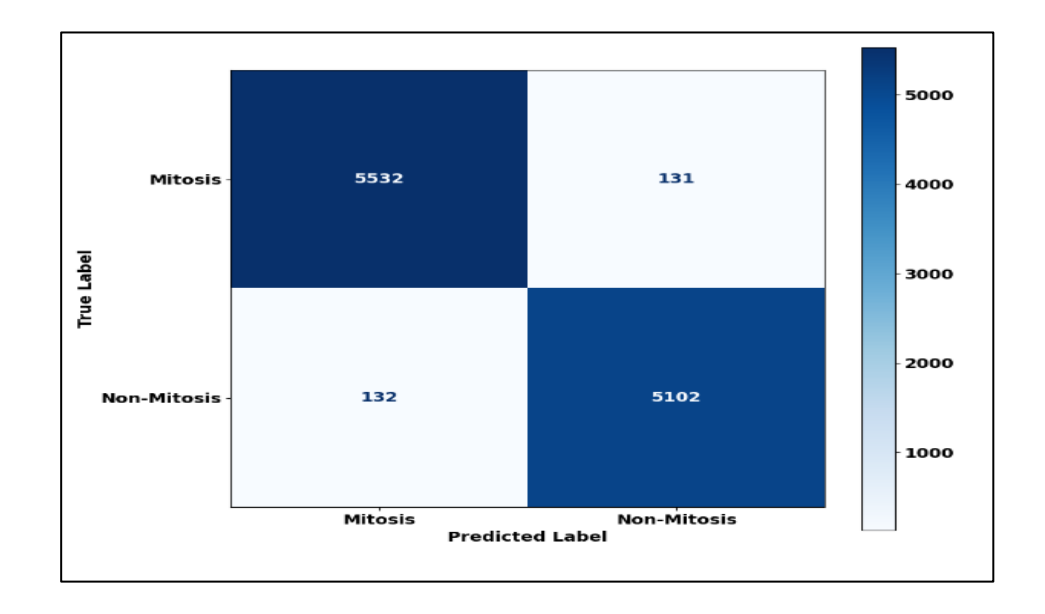


Figure 12. Confusion Matrix

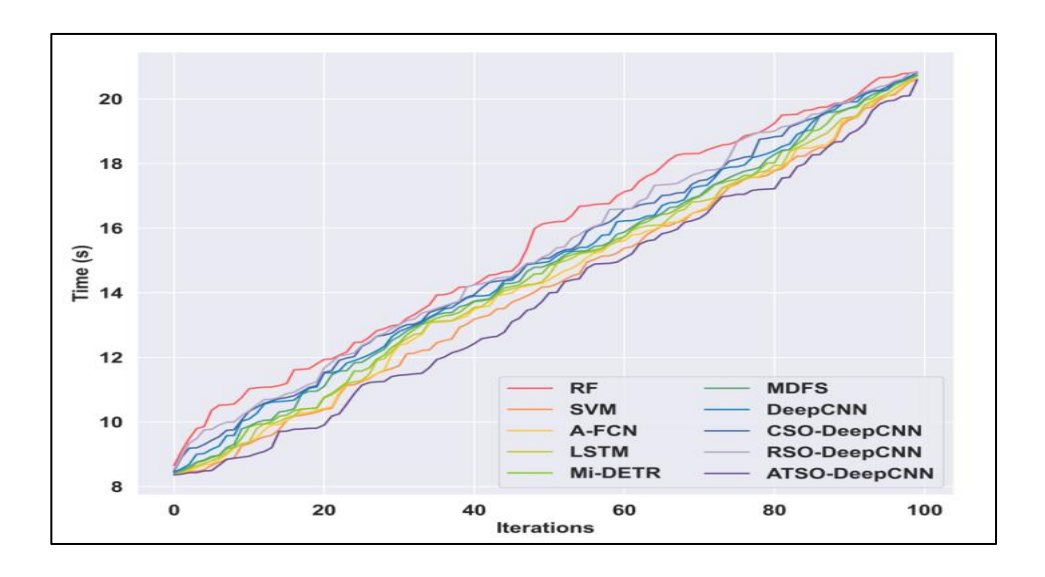


Figure 13. Computational Complexity

4.11 Ablation Study

The fused feature extraction using the DpMIE-Net feature descriptor is incorporated into the MobileNetV2, InceptionV3, and EfficientNet models, which helps to extract complex and intricate patterns from the segmented images. The evaluation of these models attained accuracies of 0.92%, 0.92%, and 0.91% respectively, which shows the effectiveness of extracting significant features for accurate mitosis classification. Figure 14 depicts the effectiveness of the individual feature extraction models.

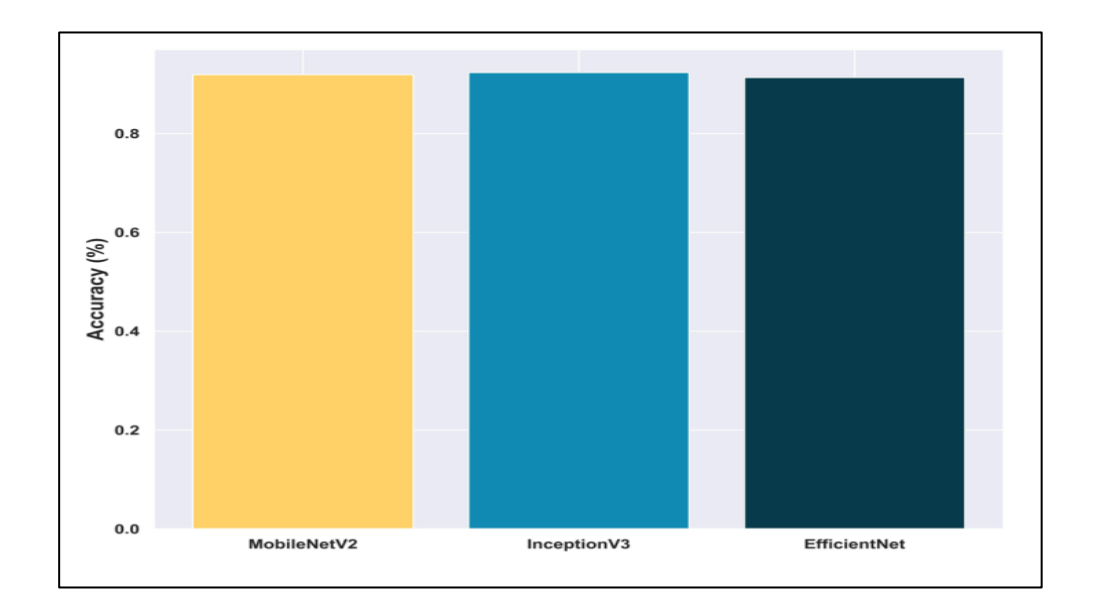


Figure 14. Ablation Study

4.12 Convergence Analysis

The proposed ATSO algorithm is analyzed based on the loss function and compared with other optimizations over 100 epochs to reduce the loss during performance. Specifically, the proposed ATSO algorithm attained a minimum loss value of 0.00001 at the 10th epoch, which explains the effectiveness of the proposed ATSO algorithm. Moreover, the remaining optimization techniques required more iterations to achieve the minimum loss. Fig. 15 illustrates the performance of the ATSO algorithm compared to other existing algorithms in terms of the loss function.

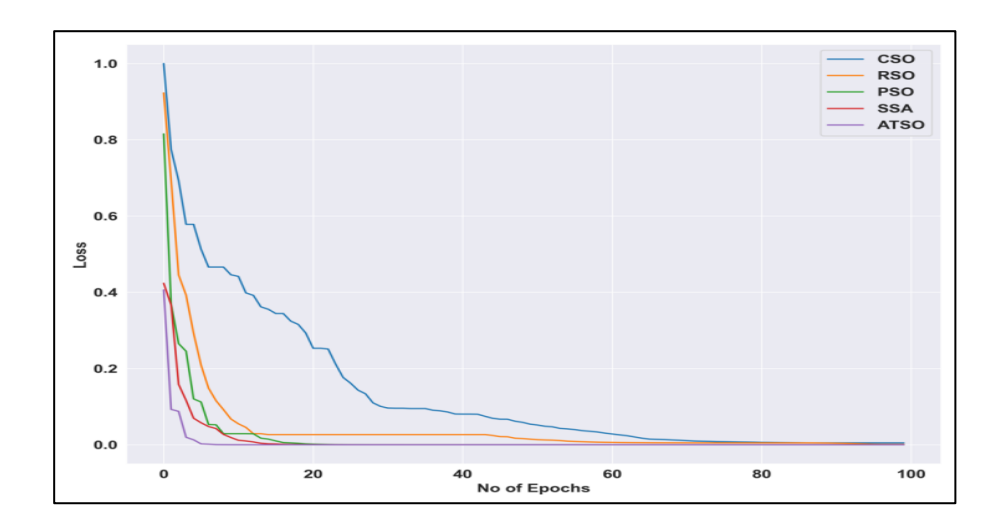


Figure 15. Convergence Analysis

4.13 Error Analysis

The Error analysis of the proposed ATSO Deep CNN model is compared with other existing models conducted across 100 epochs. The proposed model achieved a minimum loss

of 0 at the 99th epochs, and the Deep CNN attained a loss of 0.003 at the 100th epochs. Similarly, the CSO-Deep CNN and RSO-Deep CNN models achieved a minimum loss of 0 at the 100th epoch. More specifically, the mitosis classification of the proposed model reduces errors and enhances classification accuracy. Figure 16 depicts the error analysis of the proposed ATSO Deep CNN model compared with other existing models.

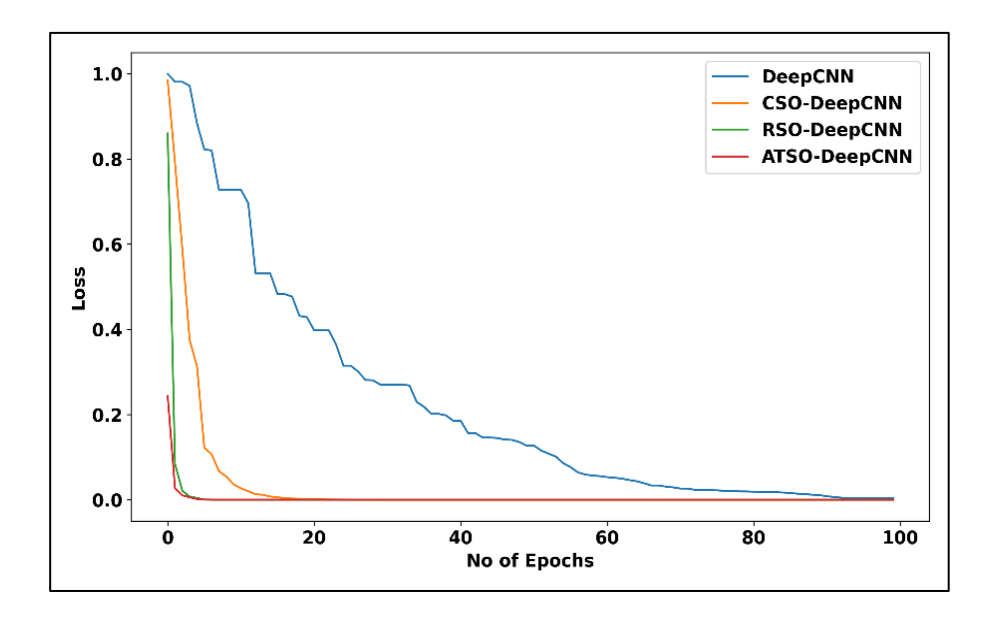


Figure 16. Error Analysis

5. Conclusion

The detection of mitotic cells and their counting using histopathological image results is an important factor in assessing the risk of metastasis. This research developed the proposed ATSO-Deep CNN model to detect mitotic cells using histopathological images. Moreover, it considers segmentation and feature fusion mechanisms that adaptively tackle the challenges associated with medical images. The segmentation with the U-Net model yields informative patterns for mitosis classification, leading to high accuracy in the segmentation process. The utilization of fused feature extraction through DpMIE-Net yields the best performance with the MITOS-ATYPIA-14 and BreCaHAD datasets. It also computes pixel-wise values, which perform better with a smaller volume of training data. The Deep CNN classifier effectively learns complex patterns and reduces overfitting, enhancing the performance of the model for mitosis classification. The incorporation of the proposed Deep CNN model with the hybrid ATSO algorithm provides a faster convergence rate and tends to create optimal solutions, improving the accuracy rate and reducing errors. More specifically, the proposed ATSO-Deep CNN model achieved better performance in terms of an accuracy of 96.31%, an F1-score of 96.3%, a precision of 96.84%, and a recall of 95.78% with a 90% training percentage for the BreCaHAD dataset. Moreover, the future direction of work will include a hybrid deep-learning classifier for better mitosis classification and grading of mitosis with histopathological images.

Statements and Declarations

Funding

"The authors declare that no funds, grants, or other support were received during the preparation of this manuscript."

Competing Interests

"The authors have no relevant financial or non-financial interests to disclose."

Author Contributions

"All authors contributed to the study conception and design. Material preparation, data collection and analysis were performed by Ms.Jithy Lijo. The first draft of the manuscript was written by Ms.Jithy Lijo and all authors commented on previous versions of the manuscript. All authors read, reviewed corrected and approved the final manuscript."

Ethics Approval

"For this type of study, ethics approval is not required".

Consent to Participate

"For this type of study, informed consent is not required".

Consent to Publish

"For this type of study, informed consent is not required".

References

- [1] Lei, Haijun, Shaomin Liu, Ahmed Elazab, Xuehao Gong, and Baiying Lei. "Attention-guided multi-branch convolutional neural network for mitosis detection from histopathological images." IEEE Journal of Biomedical and Health Informatics 25, no. 2 (2020): 358-370.
- [2] Çayır, Sercan, Gizem Solmaz, Huseyin Kusetogullari, Fatma Tokat, Engin Bozaba, Sencer Karakaya, Leonardo Obinna Iheme et al. "MITNET: a novel dataset and a two-stage deep learning approach for mitosis recognition in whole slide images of breast cancer tissue." Neural Computing and Applications 34, no. 20 (2022): 17837-17851.
- [3] Li, Chao, Xinggang Wang, Wenyu Liu, and Longin Jan Latecki. "DeepMitosis: Mitosis detection via deep detection, verification and segmentation networks." Medical image analysis 45 (2018): 121-133.
- [4] Ludovic, Roux, Racoceanu Daniel, Loménie Nicolas, Kulikova Maria, Irshad Humayun, Klossa Jacques, Capron Frédérique, Genestie Catherine, and Le Naour Gilles. "Mitosis detection in breast cancer histological images An ICPR 2012 contest." Journal of pathology informatics 4, no. 1 (2013): 8.

- [5] Nemati, Nooshin, Refik Samet, Emrah Hancer, Zeynep Yildirim, and Mohamed Traore. "A mitosis detection and classification methodology with yolov5 and fuzzy classifiers." In Proceedings of the 9th World Congress on Electrical Engineering and Computer Systems and Sciences (EECSS), vol. 111. 2023.
- [6] Tan, Xiao Jian, Nazahah Mustafa, Mohd Yusoff Mashor, and Khairul Shakir Ab Rahman. "Automated knowledge-assisted mitosis cells detection framework in breast histopathology images." Math. Biosci. Eng 19, no. 2 (2022): 1721-1745.
- [7] Kausar, Tasleem, Mingjiang Wang, M. Adnan Ashraf, and Adeeba Kausar. "SmallMitosis: small size mitotic cells detection in breast histopathology images." IEEE Access 9 (2020): 905-922.
- [8] Sebai, Meriem, Tianjiang Wang, and Saad Ali Al-Fadhli. "PartMitosis: a partially supervised deep learning framework for mitosis detection in breast cancer histopathology images." IEEE Access 8 (2020): 45133-45147.
- [9] Mahmood, Tahir, Muhammad Arsalan, Muhammad Owais, Min Beom Lee, and Kang Ryoung Park. "Artificial intelligence-based mitosis detection in breast cancer histopathology images using faster R-CNN and deep CNNs." Journal of clinical medicine 9, no. 3 (2020): 749.
- [10] Siddique, Nahian, Paheding Sidike, Colin Elkin, and Vijay Devabhaktuni. "U-Net and its variants for medical image segmentation: theory and applications." arXiv preprint arXiv:2011.01118 (2020).
- [11] Sebai, Meriem, Xinggang Wang, and Tianjiang Wang. "MaskMitosis: a deep learning framework for fully supervised, weakly supervised, and unsupervised mitosis detection in histopathology images." Medical & Biological Engineering & Computing 58, no. 7 (2020): 1603-1623.
- [12] Alom, Md Zahangir, Theus Aspiras, Tarek M. Taha, T. J. Bowen, and Vijayan K. Asari. "MitosisNet: end-to-end mitotic cell detection by multi-task learning." IEEE Access 8 (2020): 68695-68710.
- [13] Ardaç, Fatma Betül Kara, and Pakize Erdogmus. "Mi-DETR: For Mitosis Detection From Breast Histopathology Images an Improved DETR." IEEE Access (2024).
- [14] MITOS-ATYPIA-14 dataset, https://mitos-atypia-14.grand-challenge.org/Dataset/
- [15] BreCaHAD Dataset, 'https://www.kaggle.com/datasets/truthisneverlinear/brecahad".
- [16] Misra, Siddharth, Hao Li, and Jiabo He. Machine learning for subsurface characterization. Gulf Professional Publishing, 2019.
- [17] Mahawan, I. Made Avendias, and I. Putu Agus Eka Darma Udayana. "Implementation of Average Filter and Median Filter for OCR Pre Processing of Incoming Letters Image." In IOP Conference Series: Materials Science and Engineering, vol. 846, no. 1, p. 012021. IOP Publishing, 2020.
- [18] Naveed, Muhammad, Fahim Arif, Syed Muhammad Usman, Aamir Anwar, Myriam Hadjouni, Hela Elmannai, Saddam Hussain, Syed Sajid Ullah, and Fazlullah Umar. "A Deep Learning-Based Framework for Feature Extraction and Classification of Intrusion

- Detection in Networks." Wireless Communications and Mobile Computing 2022, no. 1 (2022): 2215852.
- [19] Lin, Chunmian, Lin Li, Wenting Luo, Kelvin CP Wang, and Jiangang Guo. "Transfer learning based traffic sign recognition using inception-v3 model." Periodica Polytechnica Transportation Engineering 47, no. 3 (2019): 242-250.
- [20] Atila, Ümit, Murat Uçar, Kemal Akyol, and Emine Uçar. "Plant leaf disease classification using EfficientNet deep learning model." Ecological Informatics 61 (2021): 101182.
- [21] Albashish, Dheeb, Rizik Al-Sayyed, Azizi Abdullah, Mohammad Hashem Ryalat, and Nedaa Ahmad Almansour. "Deep CNN model based on VGG16 for breast cancer classification." In 2021 International conference on information technology (ICIT), IEEE, 2021, 805-810.
- [22] Ahmed, Aram M., Tarik A. Rashid, and Soran Ab M. Saeed. "Cat swarm optimization algorithm: a survey and performance evaluation." Computational intelligence and neuroscience 2020, no. 1 (2020): 4854895.
- [23] Toolabi Moghadam, Ali, Morteza Aghahadi, Mahdiyeh Eslami, Shima Rashidi, Behdad Arandian, and Srete Nikolovski. "Adaptive rat swarm optimization for optimum tuning of SVC and PSS in a power system." International Transactions on Electrical Energy Systems 2022, no. 1 (2022): 4798029.
- [24] Mallick, Partho, Mourani Sinha, Jayanta Poray, Aiswaryya Banerjee, Souvik Sarkar, and Anupam Ghosh. "Recognition of altered gene-gene interaction using bilstm in different stages of lung adenocarcinoma." Procedia Computer Science 235 (2024): 1213-1221.